TNFalpha-signaling in drug-induced liver injury

Fredriksson, L.E.

4

Translation initiation factor EIF4A1 determines TNFα-mediated apoptosis in drug-induced liver injury through the stress protein CHOP

Lisa Fredriksson*, Bram Herpers*, Steven Wink, Giulia Benedetti, Hans de Bont, Erik Danen, Mirjam Luijten, Marjo de Graauw, John Meerman and Bob van de Water

Submitted to Hepatology

ABSTRACT

Drug-induced liver injury (DILI) is an important clinical problem. Here we used a functional genomics approach to establish the critical drug-induced toxicity pathways that act in synergy with the pro-inflammatory cytokine tumor necrosis factor α (TNFα) to cause apoptosis of liver HepG2 cells. Transcriptomics-based analysis of the toxicity response pathways activated by diclofenac (DCF), carbamazepine (CBZ), ketoconazole and nefazodone revealed activation of death-receptor/apoptosis pathway signaling, nuclear factor-erythroid 2 (NF-E2)-related factor 2 (Nrf2) oxidative stress response, and endoplasmic reticulum (ER) stress/translational initiation signaling, independent of TNFα signaling. Systematic siRNA-mediated knockdown of the individual toxicity pathway determinants established the critical role of caspase-8, Bid, Bim and APAF1 for the drug/TNFα-induced apoptosis. Cell death involved an oxidative stress component since pre-induction of the Nrf2 pathway by knockdown of its negative regulator Kelch-like ECH-associated protein 1 (Keap1) suppressed the drug/TNFα synergy and down-regulation of the glutathione reductase and peroxidase enhanced cell killing independent of TNFα. While ER stress signaling through inositol-requiring enzyme 1-alpha (IRE1α) and activating transcription factor 6 (ATF6) acted cytoprotective, CBZ- and DCF-induced activation of protein kinase R-like ER kinase (PERK) and subsequent expression of C/EBP-homologous protein (CHOP) was crucial in the onset of drug/TNFα-induced apoptosis independent of drug-induced oxidative stress. CBZ and DCF caused a strong expression of the translational initiation factor EIF4A1. Importantly, depletion of EIF4A1 almost completely inhibited CHOP expression in association with protection against the drug/TNFα-mediated cell killing. Conclusion: We propose a model in which enhanced drug-induced translation initiates PERK-mediated CHOP signaling thereby sensitizing towards caspase-8-dependent TNFα-induced apoptosis.

INTRODUCTION

Drug-induced liver injuries (DILIs) constitute an important problem both in the clinic as well as during drug development (1). The underlying cellular mechanisms that determine the susceptibility towards developing DILI are incompletely understood. Recent data indicate that the crosstalk between drug reactive metabolite-mediated intracellular stress responses and cytokine-mediated pro-apoptotic signaling are important components in the pathophysiology of DILI (2,3). Tumor necrosis factor-α (TNFα) severely enhances liver damage caused by various xenobiotics (2,4-6) and it is the major cytokine to be excreted by the liver stationary macrophages (Kupffer cells) upon exposure to bacterial endotoxins or as a response to hepatocyte damage (7). In addition, reactive drug metabolites covalently modify cellular macromolecules leading to intracellular biochemical perturbations and the induction of various intracellular stress signaling pathways. It is likely that these stress pathways are causal for the sensitization of the crosstalk with the cytokine signaling. So far it remains unclear which toxicity pathways modulate the pro-apoptotic activity of TNFα signaling.

The Kelch-like ECH-associated protein 1 (Keap1)/ nuclear factor-erythroid 2 (NF-E2)-related factor 2 (Nrf2) pathway is important in the recognition of reactive metabolites and/or cellular oxidative stress (8). Under normal conditions Nrf2 is maintained in the cytoplasm and guided towards proteasomal degradation by Keap1 (9). Nucleophilic reactions with the redox-sensitive cysteine residues of Keap1 releases Nrf2 followed by its nuclear entry and transcriptional activation of antioxidant genes (8,10). Nrf2 signaling is critical in the cytoprotective response against reactive metabolites both in vitro and in vivo (11,12), but its role in regulating TNFα pro-apoptotic signaling relation to DILI is unclear.

The endoplasmic reticulum (ER) unfolded protein response is an adaptive stress response to ER protein overload due to enhanced translation and/or perturbed protein folding. It involves expression of molecular chaperones such as the heat shock family member HSPA5 (also known as BiP or Grp78) (13). When adaptation fails, a pro-apoptotic program to eliminate the injured cell is initiated (14). The ER stress response contains three signaling arms: the protein kinase R-like ER kinase (PERK), the activating transcription factor 6 (ATF6) and the inositol-requiring enzyme 1α (IRE1α) (13). Activation of IRE1α and ATF6 initiates protective responses, while activation of PERK leads to attenuation of global protein synthesis and favored translation of activating transcription factor 4 (ATF4) by phosphorylation of eIF2α, resulting in expression of the ATF4 downstream target gene DDIT3 encoding the C/EBP homologous protein (CHOP) (15). CHOP initiates a pro-apoptotic program by modulation of Bcl2-family proteins (13,14). The role and mechanism of ER stress in controlling DILI in relation to TNFα-induced apoptosis and its relation to drug-induced oxidative stress remains undefined.

We show that different hepatotoxic drugs including diclofenac, carbamazepine, and ketoconazole show a synergistic apoptotic response with the pro-inflammatory cytokine TNFα. Genome-wide transcriptomics analysis revealed an activation of the Nrf2-

related oxidative stress response, the ER stress response as well as the death receptor-signaling pathway as critical cell toxicity pathways independent of, and preceding TNFα-mediated cell killing. A systematic short interfering RNA (siRNA) mediated knockdown approach of genes related to these stress-induced pathways allowed a detailed functional evaluation of the mechanism by which oxidative stress, ER stress and translational regulation are interrelated in the sensitization towards pro-apoptotic TNFα signaling during DILI.

MATERIALS AND METHODS

Reagents and antibodies

Diclofenac sodium, carbamazepine, nefazodone and ketoconazole were obtained from Sigma (Zwijndrecht, the Netherlands). Methotrexate was from Acros Organics (Geel, Belgium). Human recombinant TNFα was acquired from R&D Systems (Abingdon, United Kingdom). AnnexinV-Alexa633 was made as previously described (16). The antibody against caspase-8, cleaved PARP, and CHOP were from Cell Signaling (Bioké, Leiden, Netherlands). The antibody against tubulin was from Sigma and the antibody against P-Thr 981-PERK was from Santa Cruz (Tebu-Bio, Heerhugowaard, the Netherlands). The antibody against Nrf2 was a kind gift from Dr. Goldring (Liverpool University, United Kingdom).

Cell line

Human hepatoma HepG2 cells were obtained from American Type Culture Collection (ATCC, Wesel, Germany), cultured in DMEM supplemented with 10 % (v/v) FBS, 25 U/mL penicillin and 25 μg/mL streptomycin and used for experiments between passage 5 and 20.

RNA isolation and cRNA microarrays

After drug exposure for 8, 14 or 8 hours followed by the addition of 10 ng/mL TNFα for 6 hours, RNA was isolated from HepG2 cells using the RNeasy® Plus Mini Kit (Qiagen, Venlo, the Netherlands). RNA integrity and quality was assessed using the Agilent bioanalyser (Agilent Technologies, Palo Alto, CA, USA).

The synthesis of labeled cRNA and hybridization steps were performed by Service XS (Leiden, The Netherlands) using the Affymetrix 3' IVT-Express Labeling Kit (#901229) and the Affymetrix Human Genome U133 plus PM arrays. Scanning of the Array Plates was performed using the Affymetrix GeneTitan scanner. BRB Array Tools software (developed by Dr. Richard Simon and BRB-ArrayTools Development Team) was used to normalize the .cel data using the Robust Multichip Average (RMA) method. Significantly differentially expressed genes (p-value < 0.001) between the various experimental conditions were identified with an ANOVA test followed by calculation of the false discovery rate according to Benjamini and Hochberg (17). Classification of the selected genes according to their biological and toxicological functions was performed

using the Ingenuity Pathway Analysis (IPA®) software (Ingenuity® Systems, Redwood, CA, USA). Heatmap representations and hierarchical clustering (using Pearson correlation) were performed using the MultiExperiment Viewer software (18).

RNA interference

Transient knockdowns (72 hrs) of individual target genes were achieved using siGENOME SMARTpool siRNA reagents and siGENOME single siRNA sequences (50 nM; Dharmacon Thermo Fisher Scientific, Landsmeer, the Netherlands) with INTERFERin™ siRNA transfection reagent (Polyplus transfection, Leusden, the Netherlands). The negative controls were siGFP or mock transfection. The single siRNA sequences were used to exclude any off target effects of the SMARTpools resulting in a significant biological effect. The SMARTpool was considered on target when 2 or more of the 4 singles showed a similar significant effect. All siRNA-targeted genes can be found in Supplemental Data S5.

Cell death analysis assays

Induction of apoptosis in real time was quantified using a live cell apoptosis assay previously described (16). Briefly, binding of Annexin V-Alexa633 conjugate to apoptotic cells was followed in time by imaging every 30 minutes after drug exposure with a BD PathwayTM 855 imager (Becton Dickinson). The relative fluorescence intensity per cell area was quantified using Image ProTM (Media Cybernetics, Bethesda, MD, USA). When siRNA-based knockdown resulted in a difference in the area under cell death curve (AUC) larger than 2 standard deviations from the negative control, the effect was considered biologically significant.

Western blot analysis

Western blot analysis was essentially performed as previously described (2) using above-mentioned antibodies.

Live cell imaging of GFP-tagged proteins in HepG2 cells

Reporter HepG2 cells for Nrf2 activity (Srxn1 [mouse]) and ER-stress (HSPA5 [BiP/Grp78; human]) were generated by bacterial artificial chromosome (BAC) recombineering (19,20). Upon validation of correct C-terminal integration of the green fluorescent protein (GFP)-cassette by PCR, the BAC-GFP constructs were transfected using LipofectamineTM 2000 (Invitrogen, Breda, the Netherlands). Stable HepG2 BAC-GFP reporters were obtained by 500 μg/mL G418 selection. Prior to imaging, nuclei were stained with 100 ng/ml Hoechst 33342 in complete DMEM. The induction of Srxn1-GFP and HSPA5-GFP expression was followed for a period of 24 hours, by automated confocal imaging (Nikon TiE2000, Nikon, Amstelveen, the Netherlands). Quantification of the GFP intensity in individual cells was performed using Image ProTM.

Statistical analysis

All numerical results are expressed as the mean ± standard error of the mean (S.E.M.) and represent data from three independent experiments. The statistical analyses were made using GraphPad Prism 5.00 (GraphPad software, La Jolla, USA). Significance levels were calculated using 2-way ANOVA with Bonferroni post-test, * = P < .05, ** = P < .01, *** = P < .001.

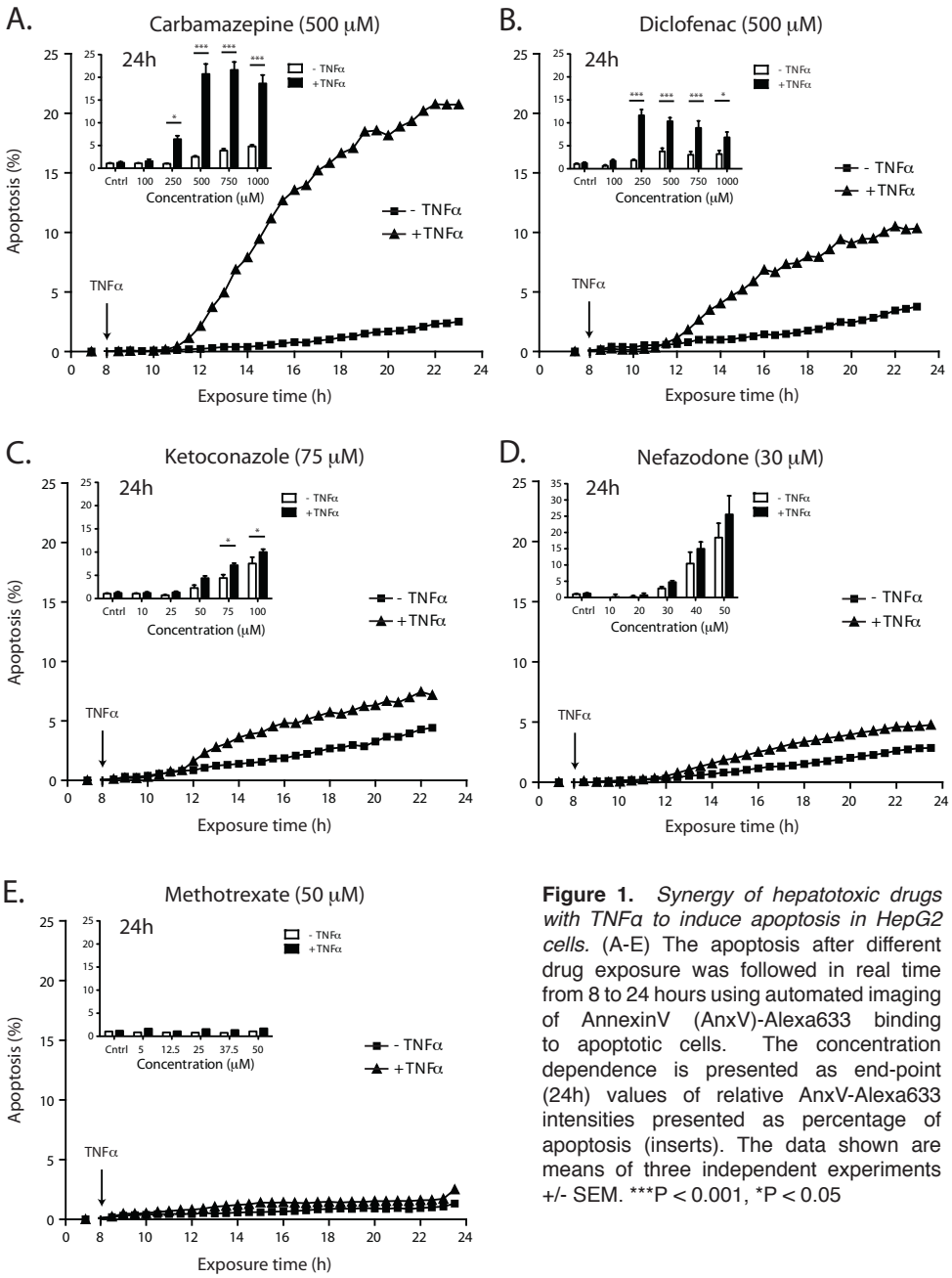

Figure 1. *Synergy of hepatotoxic drugs with TNFa to induce apoptosis in HepG2 cells.* (A-E) The apoptosis after different drug exposure was followed in real time from 8 to 24 hours using automated imaging of AnnexinV (AnxV)-Alexa633 binding to apoptotic cells. The concentration dependence is presented as end-point (24h) values of relative AnxV-Alexa633 intensities presented as percentage of apoptosis (inserts). The data shown are means of three independent experiments +/- SEM. ***P < 0.001, *P < 0.05

RESULTS

Hepatotoxic drug synergy with TNFα is preceded by oxidative stress, ER stress and death receptor signaling gene expression networks

We have previously shown that TNFα enhances the apoptosis induced by diclofenac (DCF) (2). To determine whether synergism with TNFα to induce apoptosis is a more general effect with compounds that cause drug-induced liver injury (DILI), we treated HepG2 cells for 8 hours with different compounds associated with unpredictable idiosyncratic DILI in humans, diclofenac (DCF), carbamazepine (CBZ), ketoconazole (KTZ), nefazodone (NFZ) and methotrexate (MTX), followed by an additional incubation with or without TNFα (10 ng/ml) for 16 hrs. DCF, CBZ and KTZ showed a significant enhanced apoptosis when combined with TNFα (Fig. 1 A-C). Only a trend to towards synergy was observed for NFZ (Fig. 1 D), while hardly any toxicity was observed for MTX (Fig. 1 E). Importantly, TNFα itself did not induce any apoptosis ("Control" in Fig. 1 A-E).

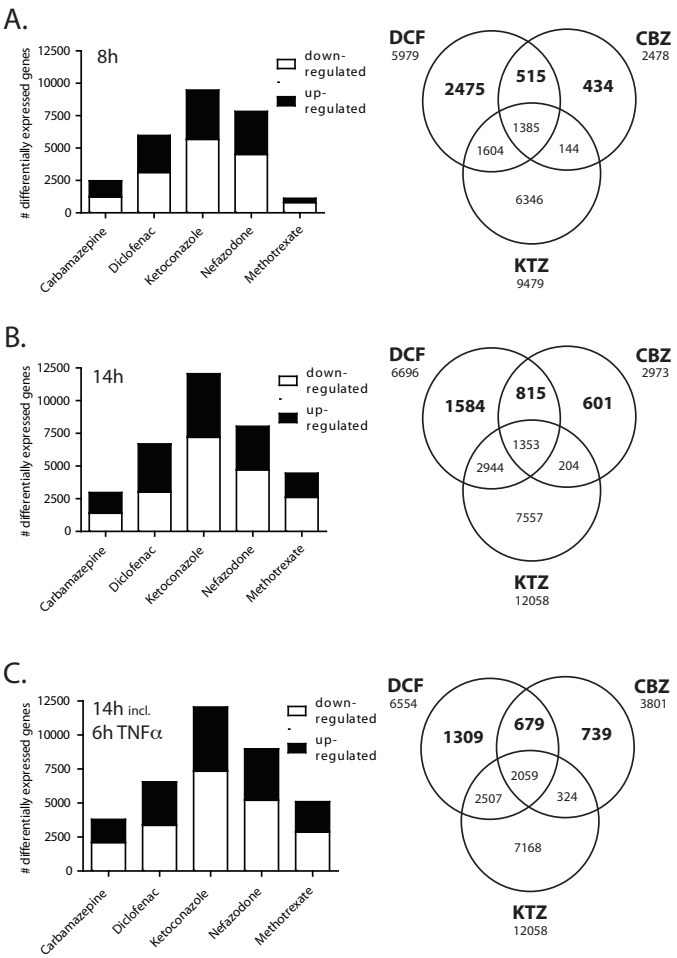

Figure 2. *Differentially expressed genes after exposure to hepatotoxic drugs.* The gene expression after 8 (A), 14 (B) and 14 hours including 6 hours of TNFα (10 ng/mL; C) exposure to diclofenac (DCF; 500 μM), carbamazepine (CBZ; 500 μM), ketoconazole (KTZ; 75 μM), nefazodone (NFZ; 30 μM) and methotrexate (MTX; 50 μM) is presented as number of genes differentially up- (black) or down-regulated (white) compared to control ($p<0.001$). The total number of genes overlapping among the TNFα-synergizing drugs is show in the corresponding Venn-diagrams.

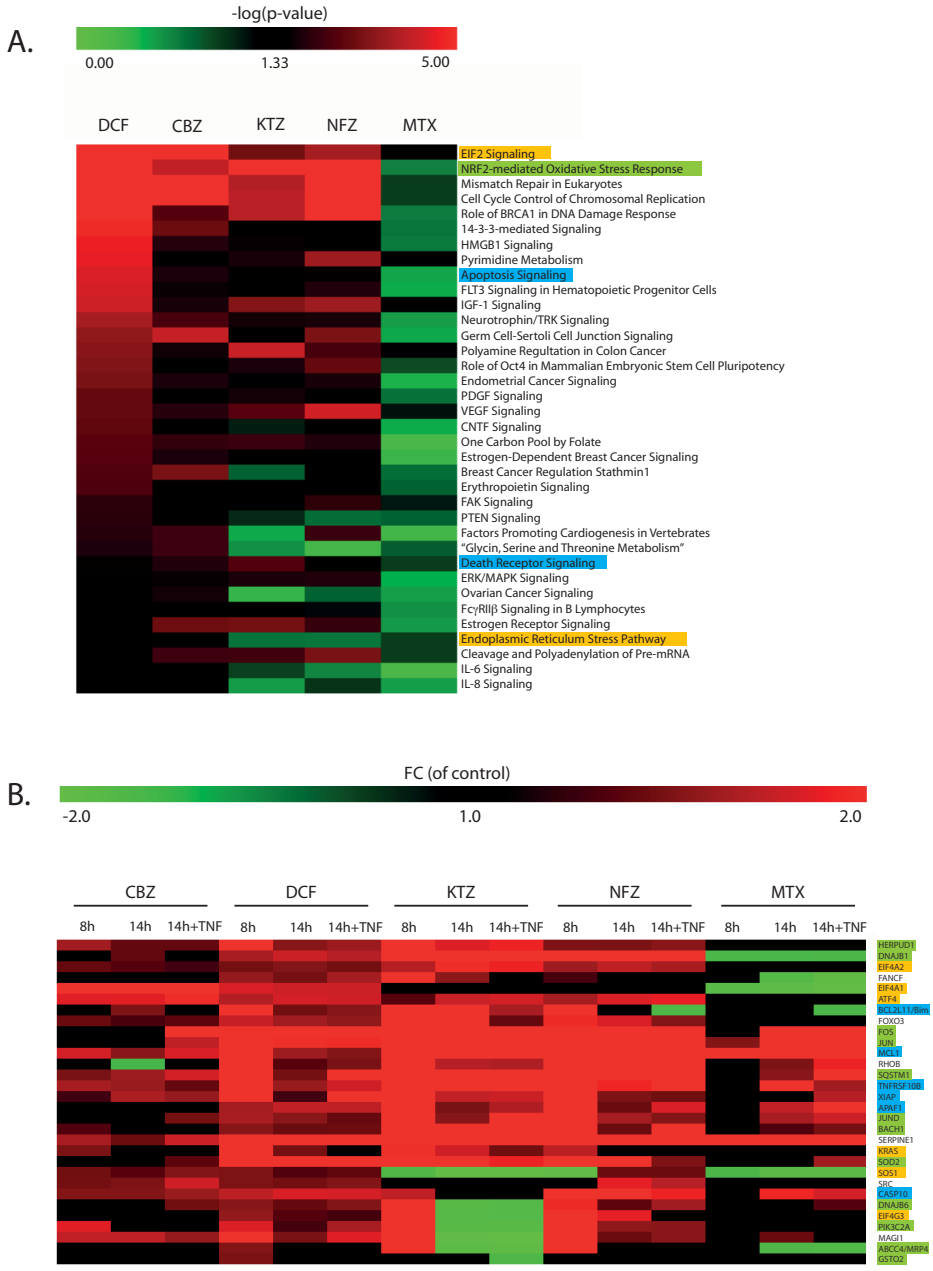

Figure 3. *Ingenuity Pathway Analysis (IPA) of common differentially expressed genes.* (A) Using IPA® the canonical pathways being significantly affected following exposure to diclofenac (DCF; 500 μM), carbamazepine (CBZ; 500 μM), ketoconazole (KTZ; 75 μM), nefazodone (NFZ; 30 μM) and methotrexate (MTX; 50 μM) for 8 hours were determined. The pathways are ranked by the criteria of being significantly regulated after DCF and CBZ, but not after MTX treatment. The most striking toxicity pathways are highlighted as follows: EIF2 Signaling/Endoplasmic Reticulum Stress Pathways are marked in yellow, Nrf2-mediated Oxidative Stress response is marked in green and Apoptosis/Death Receptor Signalling is marked in blue. (B) After hierarchical clustering using Pearson correlation and average linkage of the genes representing the pathways in A, the three clusters showing most genes up-regulated under DCF and CBZ conditions but not MTX are shown. The colours indicate the corresponding pathways from A.

To gain further insight into the toxicity pathways that may sensitize towards TNFα-mediated cell killing, we first performed a gene expression analysis on HepG2 cells exposed to DCF, CBZ, KTZ, NFZ and MTX for 8 hours (Fig. 2 A). While MTX only mildly affected the gene expression (1121 differentially expressed genes [DEGs] at 8 hours), which was related to the mild cytotoxicity (Fig. 1 E), KTZ caused the strongest gene expression changes (9479 DEGs at 8 hours; Fig. 2 A) in association with greater onset of cell death (Fig. 1 C). Not many additional changes in DEGs were observed after treatment for an additional 6 hours with the compounds either in presence or absence of TNFα (Fig. 2 B and C).

To identify likely candidate genes that contribute to this synergy we determined the overlap in DEGs for all synergizing drugs (DCF, CBZ and KTZ; see Venn-diagrams in Fig. 2). Since the most significant TNFα synergy was observed for CBZ (Fig. 1 A) we considered this a relevant model compound. DCF showed the highest overlap with CBZ in DEGs (Fig. 2 A-C). Due to this and the fact that KTZ showed marked cytotoxicity with the compound alone accompanied by only a slight, though significant, synergism with TNFα, we chose to focus on CBZ and DCF alone from here onwards.

Next we employed Ingenuity Pathway Analysis (IPA®) software to identify the signaling pathways that were affected by both CBZ and DCF (Fig. 3 A). Three prominent toxicity pathways were found: “EIF2-signaling/Endoplasmic reticulum stress pathway”, “Nrf2-mediated oxidative stress response”, and “Apoptosis/Death receptor signaling”. Subsequently we identified all the individual genes that determined these significant pathways (Supporting Data S1). Hierarchical clustering of these selected genes allowed identification of three main gene clusters that were up-regulated after 8 hours CBZ and/or DCF but not MTX treatment (Supporting Data S2). Interestingly, these contained almost exclusively genes representing the above-mentioned significantly affected pathways (compare Fig. 3 A and Supporting Data S2). For further gene selection we used a threshold of 1.5-fold change for any CBZ or DCF treatment time point (Fig. 3 B). Importantly, we confirmed the regulation of the Nrf2-mediated stress response and ER stress by DCF in primary hepatocytes (Supporting Data S3).

The death receptor pathway is critical in the drug/TNFα-induced apoptosis

Previously we showed that DCF/TNFα-induced apoptosis is dependent on the death receptor pathway (2). Next we systematically analyzed whether the CBZ/TNFα-induced apoptosis was using an identical apoptotic pathway. We observed the 41/43 kDa cleavage products of caspase-8, the most proximal initiator caspase downstream of the death receptor signaling complex, in CBZ/TNFα conditions already at 12 hours, but not for CBZ alone (Fig. 4 A). This correlated with the cleavage of caspase-3 substrate PARP (Fig. 4 A). Importantly, successful siRNA-mediated knockdown of caspase-8 (Supporting Data S4 A and S5) demonstrated that CBZ/TNFα-induced apoptosis was almost fully dependent on caspase-8 (Fig. 4 B).

Next we investigated the functional roles of the genes in the apoptotic and

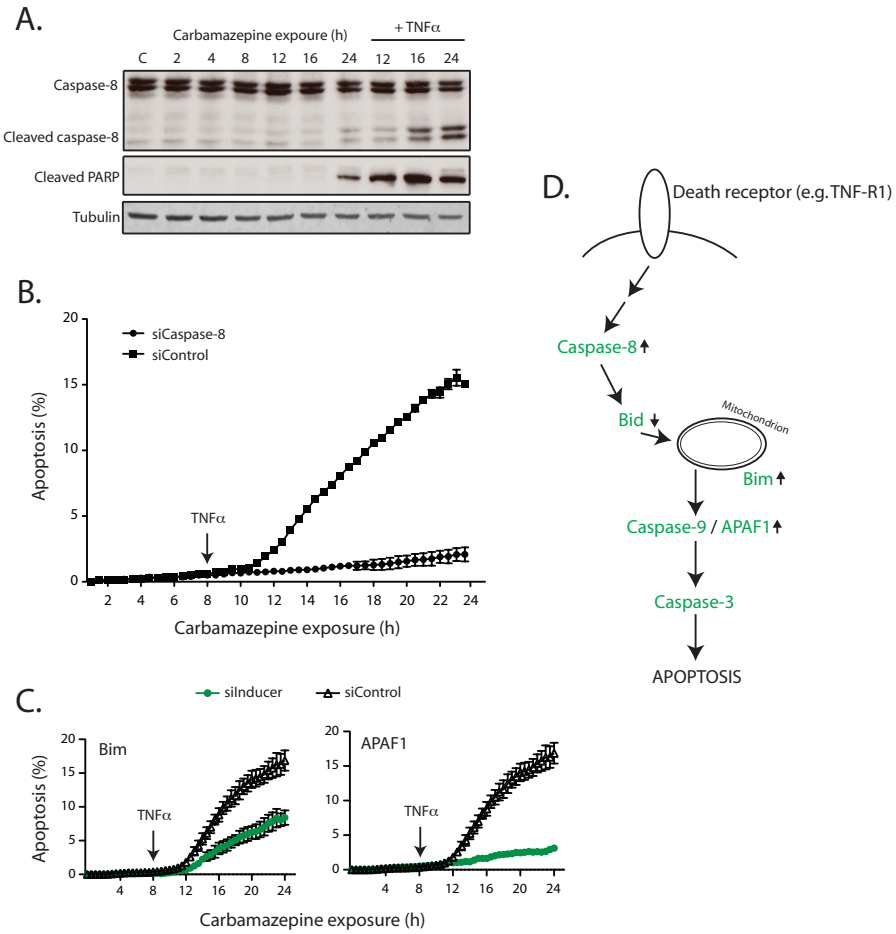

Figure 4. *Carbamazepine (CBZ)/TNFα-induced apoptosis is dependent on the extrinsic apoptotic pathway.* (A) Caspase-8 and PARP cleavage after exposure to CBZ +/- TNFα after 8 hours of exposure was assessed by western blot analysis. "C", controls exposed to vehicle for 12 hours. (B) Apoptosis was followed by AnnexinV (AnxV)-Alexa633 binding to apoptotic cells using automated microscopy after siRNA-mediated knockdown of caspase-8 and CBZ/TNFα-exposure. (C) AnxV-Alexa633 staining followed in time after knockdown of APAF1 and Bim/BCL2L11 and CBZ/TNFα-exposure. (D) Schematic representation of the pro-apoptotic pathway activated by CBZ/TNFα-exposure. Identified inducers of apoptosis are shown in green and the arrows indicate an up-or down-regulation after DCF and/or CBZ exposure on a transcriptional level (p-value ≤ 0.001) after 8 hours exposure. The data are presented as means of three independent experiments +/- SEM.

death receptor-related pathways that were up-regulated after both DCF and CBZ exposure conditions (see Fig. 3 B, blue highlight) using siRNA-mediated knockdowns of the individual genes. Knockdown of Bim/BCL2L11, a BH3 domain-containing Bcl2-family member, significantly decreased CBZ/TNFα apoptosis (Fig. 4 C). In addition, knockdown of apoptotic protease activating factor 1 (APAF1), a critical component of the apoptosome formed upon mitochondrial release of cytochrome c, led to an inhibition of apoptosis (Fig. 4 C and Supporting Data S5). We anticipated that the onset of apoptosis followed a caspase-8/Bid/APAF1/caspase-9/caspase-3 route. Indeed, knockdown of Bid, caspase-9 and caspase-3 all significantly decreased CBZ/TNFα-induced apoptosis

(Supporting Data S4 B). Collectively, these data support the involvement of the death receptor/apoptotic pathway in the induction of CBZ/TNFα-induced apoptosis (Fig. 4 D) and is therefore similar to DCF/TNFα-mediated apoptosis (2).

Oxidative stress sensitizes in the diclofenac and carbamazepine mediated apoptosis

The Nrf2-mediated oxidative stress response was significantly affected by CBZ and DCF treatment (Fig. 3), likely in relation to the formation of reactive metabolites of these compounds in our cell model (2). Modification of critical cysteine residues on Keap1, leads to the liberation of Nrf2 followed by its nuclear translocation and transcriptional activation of antioxidant genes (8,10,21). We first investigated the Nrf2 levels after CBZ and DCF treatment. DCF caused a stabilization of Nrf2, which was associated with increased levels of the Nrf2 target gene γGCSm (Fig. 5 A). Little effect of CBZ was observed on Nrf2 levels. Sulfiredoxin 1 (Srxn1) is a direct target of Nrf2 (22) and we monitored the activity of Nrf2 using live cell imaging of a BAC-Srnx1-GFP HepG2 reporter cell line. Srxn1-GFP expression was near absent under control conditions but increased over time following DCF and CBZ treatment independent of TNFα (Fig. 5 B and C). Importantly, siRNA-mediated knockdown of Nrf2 completely inhibited the Srnx1-GFP expression after CBZ, supporting Nrf2 activation (Fig. 5 C).

The antioxidant N,N'-diphenylbenzene-1,4-diamine (DPPD) drastically decreased both CBZ and CBZ/TNFα-mediated cell death (Fig. 5 D) as well as for DCF and DCF/TNFα treatment (Supporting Data S6 A), indicating a role for oxidative stress in drug/TNFα-induced apoptosis. The Nrf2 pathway and its related gene targets identified in the CBZ and DCF stress response (Fig. 3 B, green highlight) were also critically involved in the protection against drug/TNFα-mediated cell killing. Knockdown of Keap1 led to enhanced protein levels of Nrf2 (Supporting Data S6 B), which was associated with a protection against CBZ/TNFα- and DCF/TNFα-induced cytotoxicity (CBZ: Fig. 5 E and DCF: Supporting Data S7). Importantly, knockdown of Nrf2 itself (Supporting Data S6 B) led to enhancement of the apoptosis (Fig. 5 E and Supporting Data S7). In addition, depletion of two key antioxidant enzymes GSR and GPX4 that are involved in the detoxification of reactive oxygen species, led to enhancement of the cytotoxic response following drug/TNFα-exposure (Fig. 5 E). In contrast, depletion of a negative regulator of Nrf2-dependent transcription, BACH1 (23,24), which was found up-regulated following CBZ and DCF exposure in our gene array (Fig. 3 B), had a cytoprotective effect (Fig. 5 F and Supporting Data S7). Somewhat unexpected, knockdown of the multi-drug resistance protein MRP4, the glutathione S-transferase GSTO2 and the anti-oxidant gene inducer JUND also protected against the cell killing (Fig. 5 F and Supporting Data S7). All functionally relevant antioxidant components that we tested were validated by single siRNAs (Supporting data S 5). Altogether these data indicate the functional involvement of an Nrf2-dependent antioxidative stress pathway activation to protect against CBZ/TNFα as well as DCF/TNFα induced cell death.

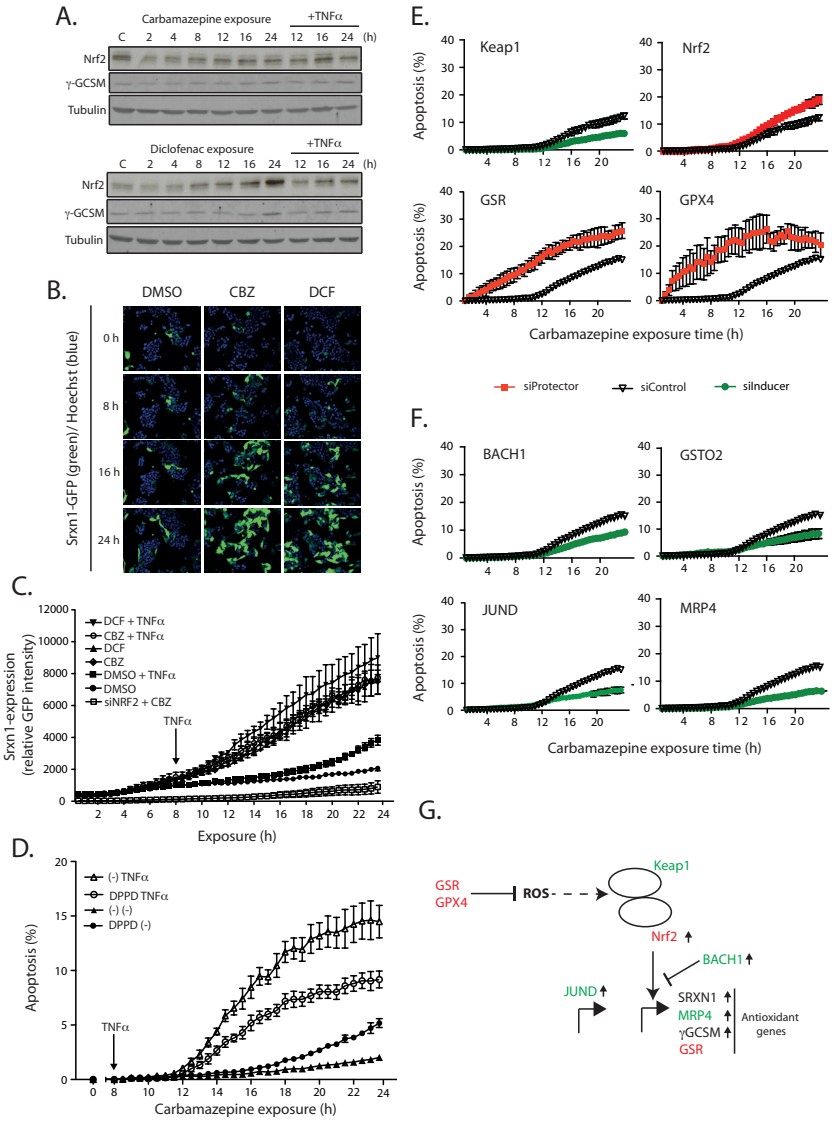

Figure 5. *Carbamazepine (CBZ) and diclofenac (DCF) induces an Nrf2-response affecting the drug/TNFα-induced apoptosis.* (A) Nrf2 and γ-GCSM protein levels were investigated by western blot analysis following DCF and CBZ exposure +/- TNFα addition. "C", controls exposed to vehicle for 12 hours. (B and C) Nrf2-responsive Srxn1-GFP levels were followed using automated confocal microscopy. Shown are representative images of Srxn1-GFP HepG2 cells exposed to vehicle (DMSO), DCF or CBZ (B) and the quantification of GFP-intensity in time normalized to the area occupied by the nuclei (Hoechst; C). (D) AnxV-Alexa633 staining of HepG2 cells +/- pre-exposure to antioxidant DPPD (10 μM) followed by CBZ-exposure +/- addition of TNFα (10 ng/mL) after 8 hours. (E) The effect on CBZ/TNFα induced apoptosis was investigated using live cell imaging of apoptosis after knockdown of crucial players in the oxidative stress response using siRNAs targeting Keap1, Nrf2, GSR and GPX4. Green indicates knockdown of inducers of oxidative stress and red protectors against oxidative stress. (F) The effect of knockdown of genes up-regulated in Fig. 3B and involved in an Nrf2-mediated oxidative stress response on the apoptosis induced by CBZ/TNFα measured by AnxV-Alexa633 staining and automated microscopy. (G) Schematic representation of the Nrf2-mediated oxidative stress response. Oxidative stress related protectors in E are shown in red, oxidative stress related inducers in F are shown in green and the arrows indicate an up-regulation on a transcriptional level (p-value ≤ 0.001) following DCF and/or CBZ exposure for 8 hours. The data are presented as means of three independent experiments +/- SEM.

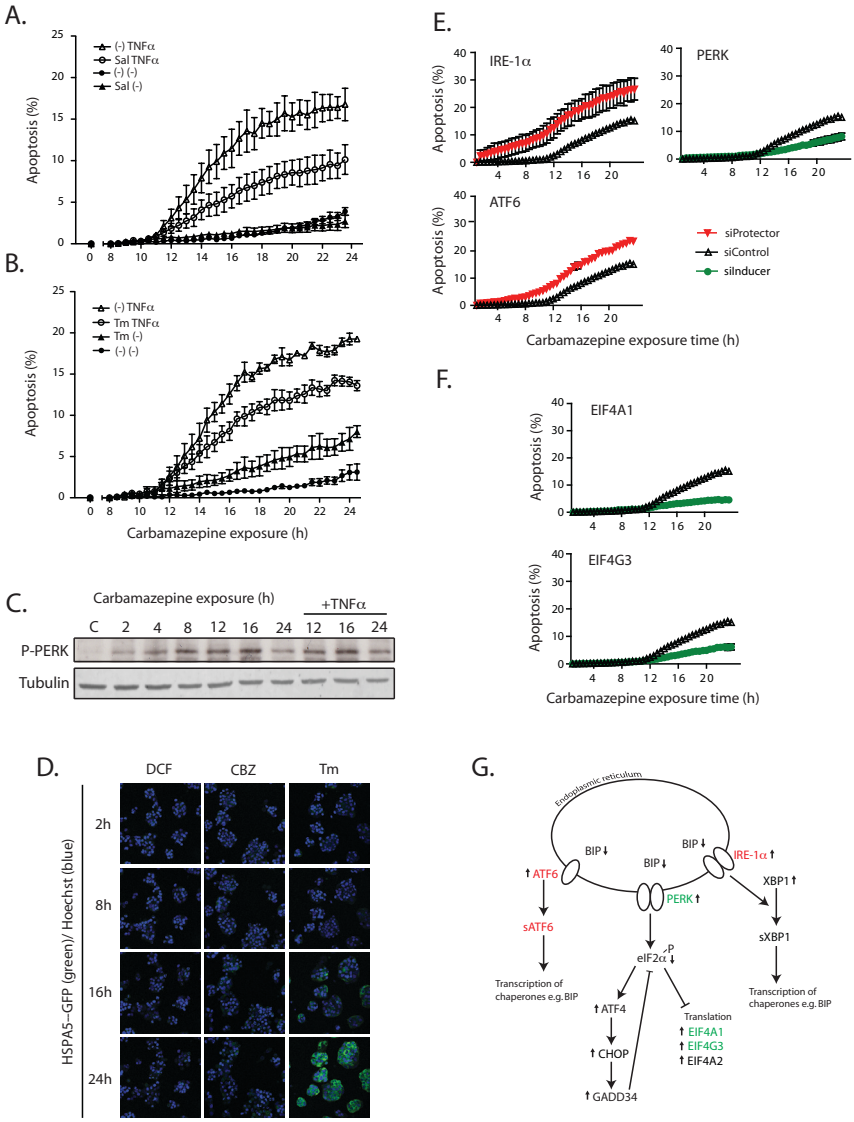

Figure 6. *Carbamazepine (CBZ) induces an ER stress-response affecting the drug/TNFα-induced apoptosis.* (A and B) HepG2 cells were pre-treated with eIF2α phosphatase inhibitor salubrinal (Sal; 50 μM; A) or ER-stressor tunicamycin (Tm; 10 μg/mL; B) for 16 hours before treatment with 500 μM CBZ. TNFα (10 ng/mL) was added 8 hours after drug exposure. (C) PERK activation was followed in time by western blotting for phosphorylated PERK (P-PERK). "C", control exposed to vehicle for 12 hours. (D) HepG2 cells expressing HSPA5-GFP (BiP) were followed in time after exposure to diclofenac (DCF; 500 μM), carbamazepine (CBZ; 500 μM), or Tm (10 μg/mL) using automated confocal microscopy. Shown are representative merged images of HSPA5-GFP (green) and Hoechst (blue) at 2, 8, 16 and 24 hours after drug exposure. (E) The effect of knockdown of the three arms of the UPR on the apoptosis induced by CBZ/TNFα was measured by AnxV-Alexa633 staining and automated microscopy. An enhanced apoptosis response is shown in red and a reduced response in green. (F) The effect of knockdown of genes involved in translational initiation (found up-regulated on expression level in Fig. 3B) on the apoptosis induced by CBZ/TNFα was measured by AnxV-Alexa633 staining and automated microscopy. (G) Schematic representation of the ER stress response. ER stress related protectors in E are shown in red, ER stress- and translation-related inducers in F are shown in green and the arrows indicate an up- or down-regulation on a transcriptional level (p-value ≤ 0.001) following DCF and/or CBZ exposure for 8 hours. The data are presented as means of three independent experiments +/- SEM.

PERK activation determines ER stress-mediated hepatotoxicant/TNF synergistic cell death

EIF2-signaling in the context of translational initiation was identified as the most significantly affected pathway by CBZ and DCF, which was associated with endoplasmic reticulum (ER) stress or unfolded protein response (UPR) pathway regulation (Fig. 3, yellow highlight). First we pre-treated cells with an inhibitor of the de-phosphorylation of eIF2α, salubrinal, thereby prolonging the translational inhibition (25). This resulted in a protection against CBZ/TNF and DCF/TNF cell death (Fig. 6 A and Supporting Data S8 A). Also pre-treatment of cells with an ER-stressor, tunicamycin, to induce a protective adaptive response (26), inhibited the apoptosis induced by CBZ/TNFα as well as DCF/TNFα (Fig. 6 B and Supporting Data S8 B). ER stress/UPR induces the activation of PERK-ATF4, IRE1α-XBP1 and ATF6 target gene expression (13). Using IPA® pathway analysis of the DEGs after 8 hours of CBZ and DCF exposure, we investigated the expression of downstream targets of ATF4, XBP1 and ATF6. ATF4 showed the strongest upregulation of downstream targets indicating an important role for PERK/ATF4 signaling (Supporting Data S9). Indeed, PERK was activated after both CBZ and DCF treatment (Fig. 6 C and Supporting Data S10). Importantly, addition of TNFα did not enhance the levels of phosphorylated PERK.

Next we systematically analyzed the critical signaling components of the ER stress/UPR in regulation of the cytotoxicity. The UPR induces expression of BiP/HSPA5 through the activation of IRE1α and ATF6 (13). Using a BAC-HSPA5-GFP reporter HepG2 cell line we demonstrated a strong induction of HSPA5 after tunicamycin treatment. Although no obvious induction was observed after CBZ and DCF (Fig. 6 D), knockdown of IRE1α and ATF6 by siRNA, sensitized cells against apoptosis, indicating a role for the IRE1α/ATF6 adaptive response in the protection against cell death (Fig. 6 E and Supporting Data S11 A). In contrast, PERK knockdown led to reduction of apoptosis-induction following CBZ/TNFα (Fig. 6 E) and DCF/TNFα (Supporting Data S11 A).

The protective effect of salubrinal suggested a central role for the translational program in the onset of apoptosis. To further test this hypothesis we performed a knockdown of the DEGs that determined the strong significance of the “EIF2 signaling” pathway (Fig. 3): the RNA helicase EIF4A1 and translation facilitator EIF4G3. Depletion of EIF4A1 and EIF4G3 provided an almost complete protection against both CBZ/TNF- and DCF/TNF-induced apoptosis (Fig. 6 F and Supporting Data S11 B). All functionally relevant ER stress-translation initiation components that we tested were validated by single siRNAs (Supporting Data S5).

Together these data support a role for the ER stress/UPR pathway and translational control in the regulation of the observed cytotoxicity (Fig. 6 G).

EIF4A1 controls CHOP expression and thereby apoptosis onset

Finally we investigated the mechanism of the PERK-mediated cytoprotection. PERK-

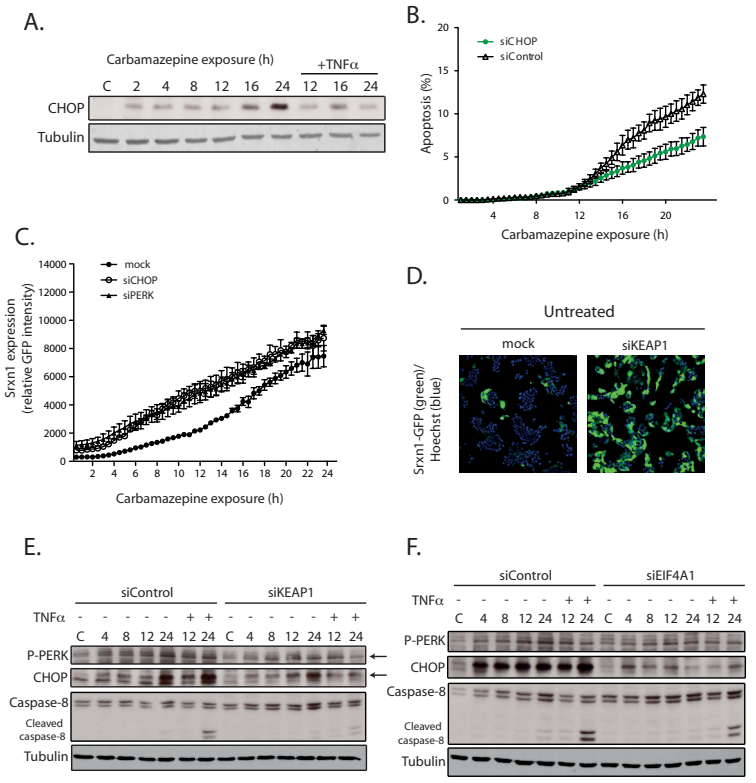

Figure 7. *CHOP-expression and apoptosis is dependent on EIF4A1.* (A) CHOP protein levels were followed in time by western blotting after CBZ (500 μM) exposure +/- addition of TNFα (10 ng/mL) after 8 hours. "C", control exposed to vehicle for 12 hours. (B) The effect of CHOP siRNA mediated knockdown on CBZ/TNFα-induced apoptosis was investigated using AnxV-labelling and automated microscopy. (C) The effect of PERK and CHOP siRNA mediated knockdown on Srxn1-GFP induction after CBZ exposure was investigated using automated confocal microscopy. GFP intensities were normalized to the area occupied by nuclei as determined by Hoechst33342 staining. (D) Shown are representative images of GFP intensity (green) after KEAP1 knockdown in Srxn1-GFP expressing HepG2 cells 72 hours after transfection under non-exposed conditions. Nuclei are labelled with Hoechst33342 (blue) (E and F) ER-stress activation, as measured by protein expression of phosphorylated PERK and CHOP using western blot, was investigated after KEAP1 (E) and EIF4A1 (F) knockdown and a time series of CBZ (500 μM) exposure +/- TNFα (10 ng/mL) addition. Cleavage of caspase-8 is shown for assessment of extrinsic apoptosis induction. Tubulin serves as loading control. "C", control exposed to vehicle for 12 hours. The data are presented as means of three independent experiments +/- SEM or representative for three independent experiments when applicable.

mediated ATF4 activation leads to expression of the pro-apoptotic transcription factor CHOP (15). In line with this, both CBZ and DCF induced the expression of CHOP in parallel to the activation of PERK (compare Fig. 6 C and 7 A and Supporting Data S10). Importantly, knockdown of CHOP strongly protected against both CBZ/TNFα and DCF/TNFα apoptosis (Fig. 7 B and Supplemental Data S11).

Since ER stress can activate the Nrf2 pathway (27) we wanted to determine the link between ER stress and oxidative stress. While PERK and CHOP knockdown protected against cell death (Fig. 6 E and 7 B), neither PERK nor CHOP knockdown inhibited the expression of the Nrf2 target gene Srxn1 (Fig. 7 C). Vice versa, knockdown of Keap1, causing stabilization of Nrf2 (Supporting Data S6 B), in association with strong

Srxn1 expression (Fig. 7 D) and cytoprotection against CBZ/TNFα and DCF/TNFα (Fig. 5 E and 7 E), did not block the activation of PERK and the expression of CHOP (Fig. 7 E).

Given the critical role of the RNA helicase EIF4A1 in the onset of apoptosis, we wondered whether the cytoprotection mediated by EIF4A1 knockdown was directly linked to the control of CHOP expression. Interestingly, EIF4A1 knockdown blocked CHOP protein expression after CBZ treatment, thereby also inhibiting activation of caspase-8 (Fig. 7 F), indicating a central role for the translational machinery in the ER stress signaling-mediated induction of CBZ/TNFα and DCF/TNFα synergy towards death receptor-mediated apoptosis.

DISCUSSION

Here we studied in detail the underlying molecular mechanisms of the synergistic apoptotic response between hepatotoxic drugs and the pro-inflammatory cytokine TNFα using transcriptomics and siRNA-mediated knockdown approaches. Using gene expression analysis of HepG2 cells exposed to different hepatotoxic drugs we identified endoplasmic reticulum stress/EIF2 signaling, Nrf2-related oxidative stress and death receptor signaling as critically activated toxicity pathways. Further functional analysis of the role of critical determinants of these pathways using siRNA approaches support a model in which drug-induced PERK/CHOP-mediated ER-stress and oxidative stress sensitizes hepatocytes to TNFα-induced pro-apoptotic signaling resulting in caspase-8 and subsequent mitochondria-dependent apoptosis (Fig. 8).

Our current data support a general role for a death receptor-mediated apoptosis pathway that act together with Bid and Bim triggered mitochondrial-mediated apoptosome activation in the CBZ and DCF mediated synergy with TNFα to induce apoptosis. At the gene expression level the death receptor signaling/apoptosis pathway was significantly regulated in DCF and CBZ treated cells, but not in cells treated with the non-toxic MTX. This included induction of caspase-8, Bim and APAF1 expression, all of which are critical in the onset of apoptosis (Fig. 4).

The hepatotoxicant/TNFα synergy is for a major part dependent on the pro-oxidant properties of both CBZ and DCF. Indeed, our gene expression profiling showed strong upregulation of Nrf2 target genes by both DCF and CBZ, which correlated with strong Nrf2-dependent induction of Srxn1. A role for DCF and/or CBZ induced oxidative stress induction is supported by gene expression data from mouse liver hepatocytes (Supplemental Data S2), and in vivo DCF treated rat liver (28) and DCF treated mouse liver (29). Importantly, both the anti-oxidant DPPD as well as knockdown of the endogenous Nrf2-inhibitor Keap1 led to protection against DCF/TNFα and CBZ/TNFα-induced apoptosis. In addition, hepatocyte cell death induced by DCF and CBZ alone are oxidative stress dependent (30,31). In our hands, the CBZ- and DCF-mediated oxidative stress was largely controlled by the glutathione peroxidase and reductase system, since knockdown of glutathione reductase (GSR) and glutathione peroxidase (GPX4) strongly enhanced the synergy-based cell killing.

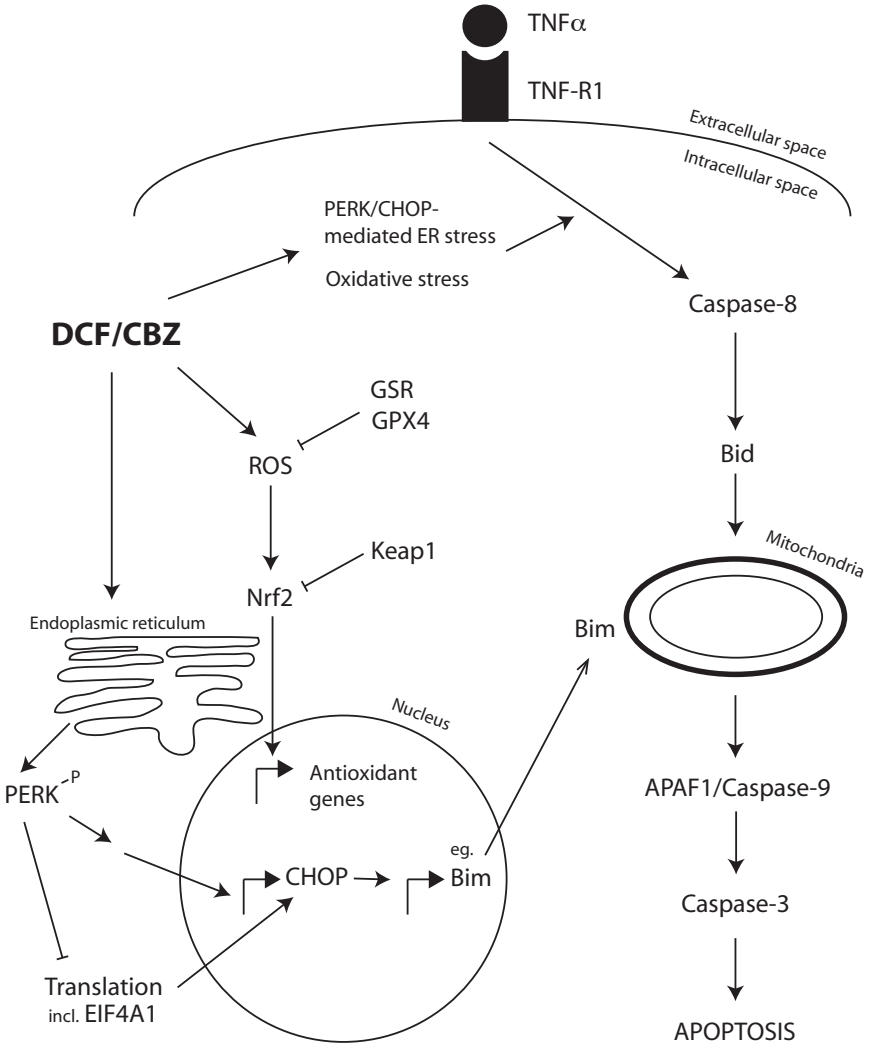

Figure 8. *Working model for drug/TNFα-induced apoptosis.* Reactive metabolites formed by diclofenac (DCF) and carbamazepine (CBZ) metabolism induce both oxidative and endoplasmic reticulum (ER) stress. The ER stress induced is solely dependent on the PERK-pathway, which results in the transcription of CHOP that in turn transcribes for example pro-apoptotic BIM. In the absence of translation less CHOP protein is expressed. Both PERK/CHOP-mediated ER stress and oxidative stress enhances the apoptotic effect of TNFα addition, an event dependent on a caspase-8 initiated Bid/Bim/APAF1/caspase-9/caspase-3 pathway.

Our data indicate that ER stress signaling through the PERK/CHOP pathway is a critical determinant for the hepatotoxicant/TNFα synergy response towards hepatocyte apoptosis. Endoplasmic reticulum (ER) stress and the UPR have been implicated in several different liver diseases including DILI (32). Here we present a more selective activation of the PERK-arm of the ER stress/UPR following DCF and CBZ exposure (Fig. 6), which was directly related to expression of CHOP (Fig. 7), a downstream target of ATF4. In contrast, we did not observe enhanced BiP (HSPA5) expression, despite the

fact that prior UPR-mediated upregulation of BiP protected against cell death. Given the critical role of CHOP in the onset of apoptosis, we propose that CHOP is a critical player in liver toxicity including sensitization for death receptor-mediated apoptosis. Upregulation of CHOP may lead to apoptosis via upregulation of pro-apoptotic Bcl-2 family members, including Bim (33). In our system Bim (BCL2L11) was up-regulated after DCF and CBZ exposure and siRNA mediated knockdown of this gene led to rescue of CBZ/TNFα and DCF/TNFα-induced cytotoxicity, thus supporting a link between ER stress-mediated CHOP induction followed by Bim expression and mitochondrial-mediated apoptosis induction.

The reduction of apoptosis after CBZ/TNFα and DCF/TNFα exposure by the use of siRNA mediated knockdown of translation initiation factors EIF4A1 and EIF4G3 and the use of an inhibitor of eIF2α dephosphorylation, salubrinal, highlight the need for translation in the hepatotoxicant-induced stress response. EIF4A1 and EIF4G3 together with cap-binding protein EIF4E are part of the EIF4F complex that unwinds secondary structures of the 5' untranslated region (UTR) of mRNA to allow ribosomal binding, scanning and thereby translation. The 5' UTR of mRNA can be more or less structured, determining its translation efficiency (34). EIF4A and EIF4G have been implicated with cap-independent translation (34). Interestingly, the translation of several anti- and pro-apoptotic genes such as XIAP, and APAF1 can occur via cap-independent mechanisms (35,36). Since depletion of EIF4A1 reduced the expression of pro-apoptotic CHOP (Fig. 7C), CHOP protein expression could be regulated by EIF4A1 cap-independent translation. While our results emphasize a role of translational control in xenobiotic toxicity, more research is required in this area.

In summary, we show that DCF and CBZ, drugs linked to idiosyncratic DILI with activation of the inflammatory system, sensitize HepG2 cells to TNFα-induced apoptosis in our in vitro system. We propose a mechanism where CBZ and DCF by inducing oxidative and PERK/CHOP-dependent ER stress, enhance the activation of the apoptotic signaling downstream of the TNF receptor, involving caspase-8, Bid, Bim and APAF1, possibly via translationally regulated induction of pro-apoptotic proteins (Fig. 8). This work sheds new light on the mechanism behind the - so far – unpredictable nature of idiosyncratic DILI. Possibly genetic polymorphisms in functionally critical determinants of the cytotoxic response are candidate susceptibility genes that predispose for idiosyncratic DILI.

ACKNOWLEDGEMENTS

We thank Harry Vrieling for kindly offering the Srxn1-GFP BAC-construct.

REFERENCES

1. Lee WM. Etiologies of acute liver failure. Semin Liver Dis 2008;28:142–152.
2. Fredriksson L, Herpers B, Benedetti G, Matadin Q, Puigvert JC, de Bont H, et al. Diclofenac inhibits tumor necrosis factor-α-induced nuclear factor-κB activation causing synergistic hepatocyte apoptosis. Hepatology 2011;53:2027–2041.
3. Roth RA, Ganey PE. Animal models of idiosyncratic drug-induced liver injury--current status. Crit Rev Toxicol 2011;41:723–739.
4. Shaw PJ, Hopfensperger MJ, Ganey PE, Roth RA. Lipopolysaccharide and trovafloxacin coexposure in mice causes idiosyncrasy-like liver injury dependent on tumor necrosis factor-alpha. Toxicol Sci 2007;100:259–266.
5. Barton CC, Barton EX, Ganey PE, Kunkel SL, Roth RA. Bacterial lipopolysaccharide enhances aflatoxin B1 hepatotoxicity in rats by a mechanism that depends on tumor necrosis factor alpha. Hepatology 2001;33:66–73.
6. Lu J, Jones AD, Harkema JR, Roth RA, Ganey PE. Amiodarone exposure during modest inflammation induces idiosyncrasy-like liver injury in rats: role of tumor necrosis factor-alpha. Toxicol Sci 2012;125:126–133.
7. Roberts RA, Ganey PE, Ju C, Kamendulis LM, Rusyn I, Klaunig JE. Role of the Kupffer cell in mediating hepatic toxicity and carcinogenesis. Toxicol Sci 2007;96:2–15.
8. Jaiswal AK. Nrf2 signaling in coordinated activation of antioxidant gene expression. Free Radic Biol Med 2004;36:1199–1207.
9. Kobayashi A, Kang M-I, Okawa H, Ohtsuji M, Zenke Y, Chiba T, et al. Oxidative stress sensor Keap1 functions as an adaptor for Cul3-based E3 ligase to regulate proteasomal degradation of Nrf2. Mol Cell Biol 2004;24:7130–7139.
10. Copple IM, Goldring CE, Kitteringham NR, Park BK. The Nrf2-Keap1 defence pathway: role in protection against drug-induced toxicity. Toxicology 2008;246:24–33.
11. Copple IM, Goldring CE, Jenkins RE, Chia AJL, Randle LE, Hayes JD, et al. The hepatotoxic metabolite of acetaminophen directly activates the Keap1-Nrf2 cell defense system. Hepatology 2008;48:1292–1301.
12. Okawa H, Motohashi H, Kobayashi A, Aburatani H, Kensler TW, Yamamoto M. Hepatocyte-specific deletion of the keap1 gene activates Nrf2 and confers potent resistance against acute drug toxicity. Biochem Biophys Res Commun 2006;339:79–88.
13. Hetz C. The unfolded protein response: controlling cell fate decisions under ER stress and beyond. Nat Rev Mol Cell Biol 2012;13:89–102.
14. Woehlbier U, Hetz C. Modulating stress responses by the UPRosome: a matter of life and death. Trends Biochem Sci 2011;36:329–337.
15. Harding HP, Novoa I, Zhang Y, Zeng H, Wek R, Schapira M, et al. Regulated translation initiation controls stress-induced gene expression in mammalian cells. Mol Cell 2000;6:1099–1108.
16. Puigvert JC, de Bont H, van de Water B, Danen EHJ. High-throughput live cell imaging of apoptosis. Curr Protoc Cell Biol 2010;Chapter 18:Unit 18.10.1–13.
17. Benjamini Y, Hochberg Y. Controlling the false discovery rate: a practical and powerful approach to multiple testing. J Royal Statist Soc, B 1995;57:289–300.
18. Saeed A, Sharov V, White J, Li J, Liang W, Bhagabati N, et al. TM4: a Free, Open-Source System for Microarray Data Management and Analysis. Biotechniques 2003;34:374–378.
19. Poser I, Sarov M, Hutchins JRA, Hériché J-K, Toyoda Y, Pozniakovsky A, et al. BAC TransgeneOmics: a high-throughput method for exploration of protein function in mammals. Nat Methods 2008;5:409–415.
20. Hendriks G, Atallah M, Morolli B, Calléja F, Ras-Verloop N, Huijskens I, et al. The ToxTracker assay: novel GFP reporter systems that provide mechanistic insight into the genotoxic properties of chemicals. Toxicological Sciences 2012;125:285–298.
21. Soriano FX, Baxter P, Murray LM, Sporn MB, Gillingwater TH, Hardingham GE. Transcriptional regulation of the AP-1 and Nrf2 target gene sulfiredoxin. Mol Cells 2009;27:279–282.
22. Soriano FX, Léveillé F, Papadia S, Higgins LG, Varley J, Baxter P, et al. Induction of sulfiredoxin expression and reduction of peroxiredoxin hyperoxidation by the neuroprotective Nrf2 activator 3H-1,2-dithiole-3-thione. J Neurochem 2008;107:533–543.
23. Oyake T, Itoh K, Motohashi H, Hayashi N, Hoshino H, Nishizawa M, et al. Bach proteins belong to a novel family of BTB-basic leucine zipper transcription factors that interact with MafK and regulate transcription through the NF-E2 site. Mol Cell Biol 1996;16:6083–6095.
24. Dhakshinamoorthy S, Jain AK, Bloom DA, Jaiswal AK. Bach1 competes with Nrf2 leading to negative regulation of the antioxidant response element (ARE)-mediated NAD(P)H:quinone oxidoreductase 1 gene expression and induction in response to antioxidants. J Biol Chem 2005;280:16891–16900.
25. Boyce M, Bryant KF, Jousse C, Long K, Harding HP, Scheuner D, et al. A selective inhibitor of eIF2alpha

dephosphorylation protects cells from ER stress. Science 2005;307:935–939.
26. van De Water B, Wang Y, Asmellash S, Liu H, Zhan Y, Miller E, et al. Distinct endoplasmic reticulum signaling pathways regulate apoptotic and necrotic cell death following iodoacetamide treatment. Chem Res Toxicol 1999;12:943–951.
27. Cullinan SB, Diehl JA. Coordination of ER and oxidative stress signaling: the PERK/Nrf2 signaling pathway. Int J Biochem Cell Biol 2006;38:317–332.
28. Deng X, Liguori MJ, Sparkenbaugh EM, Waring JF, Blomme EAG, Ganey PE, et al. Gene expression profiles in livers from diclofenac-treated rats reveal intestinal bacteria-dependent and -independent pathways associated with liver injury. J Pharmacol Exp Ther 2008;327:634–644.
29. Cantoni L, Valaperta R, Ponsoda X, Castell JV, Barelli D, Rizzardini M, et al. Induction of hepatic heme oxygenase-1 by diclofenac in rodents: role of oxidative stress and cytochrome P-450 activity. J Hepatol 2003;38:776–783.
30. Gómez-Lechón MJ, Ponsoda X, O'Connor E, Donato T, Castell JV, Jover R. Diclofenac induces apoptosis in hepatocytes by alteration of mitochondrial function and generation of ROS. Biochem Pharmacol 2003;66:2155–2167.
31. Santos NAG, Medina WSG, Martins NM, Rodrigues MAC, Curti C, Santos AC. Involvement of oxidative stress in the hepatotoxicity induced by aromatic antiepileptic drugs. Toxicol in Vitro 2008;22:1820–1824.
32. Dara L, Ji C, Kaplowitz N. The contribution of endoplasmic reticulum stress to liver diseases. Hepatology 2011;53:1752–1763.
33. Puthalakath H, O'Reilly LA, Gunn P, Lee L, Kelly PN, Huntington ND, et al. ER stress triggers apoptosis by activating BH3-only protein Bim. Cell 2007;129:1337–1349.
34. Jackson RJ, Hellen CUT, Pestova TV. The mechanism of eukaryotic translation initiation and principles of its regulation. Nat Rev Mol Cell Biol 2010;11:113–127.
35. Holcik M, Lefebvre C, Yeh C, Chow T, Korneluk RG. A new internal-ribosome-entry-site motif potentiates XIAP-mediated cytoprotection. Nat Cell Biol 1999;1:190–192.
36. Coldwell MJ, Mitchell SA, Stoneley M, MacFarlane M, Willis AE. Initiation of Apaf-1 translation by internal ribosome entry. Oncogene 2000;19:899–905.

SUPPORTING MATERIALS AND METHODS

Isolation and culture of primary mouse hepatocytes

Primary mouse hepatocytes were isolated from 8-10 weeks old male C57BL/6 mice by a modified two-step collagenase perfusion technique (collagenase type IV, Sigma-Aldrich, Zwijndrecht, The Netherlands), as described previously (1). In short, hepatocytes suspensions with at least 80 % viability were seeded onto plates coated with collagen gel and after attachment overlayed with a second layer of collagen gel, to form a sandwich configuration. Cells were kept in serum-free medium and the culture medium was changed daily until exposures were performed.

Gene expression profiling

Forty-six hours after isolation, hepatocytes were exposed to either 300 μM DCF or the solvent DMSO. After 24 hours of exposure, cells were collected in 1 ml RNAprotect (QIAgen, Venlo, The Netherlands) and stored at -80˚C for RNA isolation. RNA was extracted using QIAzol and purified using the miRNeasy mini kit and the QIAcube (Qiagen), according to the manufacturer's protocol. For both the DCF and vehicle-control groups, four biological replicates were used. RNA concentrations were measured using the NanoDrop ND-1000 Spectrophotometer (Nanodrop Technologies, Wilmington, DE, USA) and RNA quality was assessed with the Agilent 2100 Bioanalyzer (Agilent Technologies, Amstelveen, The Netherlands). Labeled RNA was prepared using the Affymetrix gene chip 3'IVT express kit and hybridized to the Affymetrix Mouse Genome 430 2.0 GeneChip arrays, according to the manufacturer's instructions. After hybridization the array chips were washed and stained with a Genechip Fluidics Station 450 and scanned using the Affymetrix gene chip scanner 3000.

Data analysis

Affymetrix CEL files were each checked on quality, including RNA degradation control, correlation and clustering. All quality checks were within acceptable limits, according to Affymetrix standards. After quality control the files were normalized with the Multichip Average (RMA) procedure (2), using the custom chip description files (CDFs) as previously described (3). For detecting significantly regulated genes, the microarray analysis of variance (MAANOVA) package in R was used (R version 2.9.2, www.r-project.org). For the analyses on significantly regulated genes per compound between treated and control samples, an F1-test was used. Gene-specific P-values were corrected with a Benjamini- Hochberg false discovery rate (FDR) with a cut-off at 0.1 (Benjamini and Hochberg, 1995).

SUPPORTING REFERENCES

1. Van Kesteren PC, Zwart PE, Pennings JL, Gottschalk WH, Kleinjans JC, et al. Deregulation of cancer-related pathways in primary hepatocytes derived from DNA repair-deficient Xpa-/-p53+/- mice upon exposure to benzo[a]pyrene. Toxicol Sci 2011:123:123-132.
2. Irizarry RA, Hobbs B, Collin F, Beazer-Barclay YD, Antonellis KJ, et al. Exploration, normalization, and summaries of high density oligonucleotide array probe level data. Biostatistics 2003:4:249-264.
3. De Leeuw WC, Rauwerda H, Jonker MJ, Breit TM. Salvaging Affymetrix probes after probe-level re-annotation. BMC Reserch Notes 2008:1:66.
4. Benjamini, Y. and Hochberg, Y. Controlling the false discovery rate: a practical and powerful approach to multiple testing. Journal of the Royal Statistical Society, Series B (Methodological). 1995;57:289–300.

Supporting Data S1. *Genes representing significantly regulated canonical signaling pathways.* The genes representing the significantly regulated canonical signaling pathways after 8 hours of diclofenac (DCF) and/or carbamazepine (CBZ) exposure as determined using the Ingenuity Pathway Analysis (IPA®) software (Fig. 3A) are presented. Up-regulated genes after CBZ and/or DCF treatment are marked in red and down-regulated genes in green. In the case of two-colored gene names, the left part represents DCF and the right CBZ.

IPA Canonical Pathways	Involved genes in DCF and CBZ at 8h
EIF2 signaling	AKT1; AKT2; EIF1; EIF5; EIF1AX; EIF2A; EIF2AK1; EIF2AK3; EIF2AK4; EIF2B1; EIF2C2; EIF2C3; EIF2C4; EIF2S1; EIF2S2; EIF3A; EIF3B; EIF3C; EIF4A1; EIF4A2; EIF4G1; EIF4G3; GSK3B; HRAS; INSR; KRAS; MRAS; NRAS; PDPK1; PIK3C2A; PIK3CA; PIK3CD; PIK3R1; PIK3R2; PIK3R3; PPP1CB; PPP1R15A; RRAS2; SOS1; SOS2
NRF2-mediated Oxidative Stress Response	ABCC4; ACTA1; AKT1; ATF4; BACH1; CBR1; CUL3; DNAJA1; DNAJA2; DNAJA3; DNAJB1; DNAJB4; DNAJB6; DNAJB9; DNAJB14; DNAJC5; DNAJC6; DNAJC7; DNAJC8; DNAJC9; DNAJC10; DNAJC11; DNAJC15; DNAJC18; DNAJC21; EIF2AK3; FOS; GCLC; GCLM; GPX2; GSK3B; GSTO2; GSTT1; HERPUD1; HRAS; JUN; JUNB; JUND; KRAS; MAFF; MAFG; MAFK; MAP2K3; MAP2K5; MAP2K6; MAP3K7; MAPK8; MAPK14; MRAS; NFE2L2; NQO1; NRAS; PIK3C2A; PIK3CA; PIK3CD; PIK3R1; PIK3R2; PIK3R3; PRKCA; PRKCI; PRKD3; PTPLAD1; RBX1; RRAS2; SOD2; SQSTM1; TXNRD1; UBE2K; USP14; VCP
Cell Cycle Control of Chromosomal Replication	CDC6; CDC7; CDK2; CDK5; CDK6; CDK7; CDT1; MCM3; MCM4; MCM5; MCM6; MCM7; ORC1; ORC6; RPA1; RPA2
Role of BRCA1 in DNA Damage Respnse	BARD1; BRIP1; CHEK1; E2F1; E2F2; E2F5; FANCB; FANCC; FANCF; FANCG; FANCL; FANCM; GADD45A; MSH2; MSH6; POU2F1; RAD50; RAD51; RBL1; RFC2; RFC3; RFC4; RFC5; RPA1; SLC19A1; STAT1; TP53
14-3-3-mediated Signaling	AKT1; AKT2; CBL; CDKN1B; FOS; FOXO1; GSK3B; HRAS; JUN; KRAS; MAPK8; MRAS; NRAS; PDCD6IP; PIK3C2A; PIK3CA; PIK3CD; PIK3R1; PIK3R2; PIK3R3; PLCD1; PLCG1; PRKCA; PRKCI; PRKD3; RPS6KA1; RRAS2; SRC; TNFRSF1A; TSC1; TUBA1A; TUBA1B; TUBA1C; TUBA3C; TUBA4A; TUBB; TUBB1; TUBB3; TUBB6; TUBB2A; TUBB2C; TUBG1; YAP1; YWHAB; YWHAQ
HMGB1 Signaling	AKT1; AKT2; FNBP1; FOS; HAT1; HMGB1; HRAS; ICAM1; IFNGR2; IL8; IL1R1; JUN; KRAS; MAP2K3; MAP2K5; MAP2K6; MAPK8; MAPK13; MAPK14; MRAS; MYST4; NRAS; PIK3C2A; PIK3CA; PIK3CD; PIK3R1; PIK3R2; PIK3R3; PLAT; RBBP7; RELA; RHOB; RHOQ; RHOT2; RHOU; RRAS2; SERPINE1; SP1; TNFRSF1A
Pyrimidine Metabolism	CMPK2; CTPS; CTPS2; DCTPP1; DPYSL2; DTYMK; DUT; ENPP1; ENTPD4; ENTPD5; ENTPD7; NME3; POLA1; POLA2; POLD1; POLD3; POLE; POLE2; POLE3; POLE4; POLG; POLH; POLK; POLQ; POLR1B; POLR1D; POLR1E; POLR2A; POLR2E; POLR2F; POLR2H; POLR2L; POLR3A; POLR3D; POLR3H; POLR3K; REV3L; RFC5; RRM1; RRM2; RRM2B; TK1; TK2; TXNRD1; TYMS; UCK1; UCK2; UNG; UPP1
Apoptosis Signaling	ACIN1; AIFM1; APAF1; BCL2L1; BCL2L11; BID; CAPN10; CASP2; CASP6; CASP8; CASP10; CYCS; DFFA; ENDOG; FAS; HRAS; HTRA2; IKBKG; KRAS; LMNA; MAP4K4; MAPK8; MCL1; MRAS; NRAS; PARP1; PLCG1; PRKCA; RELA; ROCK1; RPS6KA1; RRAS2; TNFRSF1A; TP53; XIAP
FLT3 Signaling in Hematopoietic Progenitor Cells	AKT1; AKT2; ATF2; ATF4; CBL; CREB3L4; EIF4EBP1; GAB2; HRAS; KRAS; MAPK13; MAPK14; MRAS; NRAS; PDPK1; PIK3C2A; PIK3CA; PIK3CD; PIK3R1; PIK3R2; PIK3R3; RPS6KA1; RPS6KA5; RRAS2; SOS1; SOS2; STAT1; STAT3; STAT6; STAT5B
IGF-1 Signaling	AKT1; AKT2; CSNK2A1; CSNK2A2; CYR61; FOS; FOXO1; FOXO3; GRB10; HRAS; IGF1R; IGFBP1; IGFBP3; IRS1; JUN; KRAS; MAPK8; MRAS; NEDD4; NRAS; PDPK1; PIK3C2A; PIK3CA; PIK3CD; PIK3R1; PIK3R2; PIK3R3; PRKACB; PRKCI; PTK2; RASA1; RRAS2; SOCS6; SOCS7; SOS1; SOS2; SRF; STAT3; YWHAB; YWHAQ
Neurotrophin/TRK Signaling	AKT1; ATF2; ATF4; CREB3L4; FOS; FRS2; GAB1; HRAS; JUN; KRAS; MAP2K3; MAP2K5; MAP2K6; MAPK8; MRAS; NRAS; PDPK1; PIK3C2A; PIK3CA; PIK3CD; PIK3R1; PIK3R2; PIK3R3; PLCG1; RPS6KA1; RRAS2; SOS1; SOS2
Germ-Cell-Sertoli Cell Junction Signaling	ACTA1; AGGF1; AKT1; CDH1; CTNNB1; EPN2; EPN3; FER; FNBP1; HRAS; ITGA2; ITGB1; KRAS; MAP2K3; MAP2K6; MAP3K7; MAP3K11; MAPK8; MAPK14; MRAS; NRAS; PAK2; PDPK1; PIK3C2A; PIK3CA; PIK3CD; PIK3R1; PIK3R2; PIK3R3; PTK2; RAB8B; RHOB; RHOQ; RHOT2; RHOU; RRAS2; SORBS1; SRC; TJP1; TNFRSF1A; TUBA1A; TUBA1B; TUBA1C; TUBA3C; TUBA4A; TUBB; TUBB1; TUBB3; TUBB6; TUBB2A; TUBB2C; TUBG1
Erythropietin Signaling	AKT1; AKT2; CBL; EPO; FOS; HRAS; JUN; KRAS; MRAS; NRAS; PDPK1; PIK3C2A; PIK3CA; PIK3CD; PIK3R1; PIK3R2; PIK3R3; PLCG1; PRKCA; PRKCI; PRKD3; RELA; RRAS2; SOS1; SOS2; SRC; STAT5B
FAK Signaling	ACTA1; AKT1; AKT2; ARHGAP26; ARHGEF7; ASAP1; CAPN10; GIT2; HRAS; ITGA2; ITGB1; KRAS; MRAS; NRAS; PAK2; PDPK1; PIK3C2A; PIK3CA; PIK3CD; PIK3R1; PIK3R2; PIK3R3; PLCG1; PTEN; PTK2; RRAS2; SOS1; SOS2; SRC; VCL
PTEN Signaling	AKT1; AKT2; BCL2L1; BCL2L11; CBL; CDKN1B; CSNK2A1; CSNK2A2; DDR1; FGFR1; FOXO1; FOXO3; GSK3B; HRAS; IGF1R; IKBKG; INSR; ITGA2; ITGB1; KRAS; MAGI1; MRAS; NRAS; PDPK1; PIK3CA; PIK3CD; PIK3R1; PIK3R2; PIK3R3; PTEN; PTK2; RELA; RRAS2; SOS1; SOS2
Factors Promoting Cardiogenesis in Vertebrates	ACVR1; ACVR1B; ACVR2B; ATF2; BMP4; CCNE1; CCNE2; CDC6; CDK2; CTNNB1; DKK1; FZD3; FZD4; FZD5; FZD6; FZD7; GATA4; GSK3B; HNF1A; LRP6; MAP3K7; MAPK14; PRKCA; PRKCI; PRKD3; SMAD1; SMAD2; SMAD4; SMAD9; TCF3; TCF7L2
"Glycin, Serine and Threonine Metabolism"	ALAS2; CBS; CHDH; CHKA; CHKB; CTH; DBT; ELOVL2; GARS; GLDC; GLYCTK; GOT1; MAOA; MAOB; PLCD1; PLCG1; PSAT1; PSPH; SARDH; SARS; SHMT1; SHMT2; SMOX; SRR
Death Receptor Signaling	APAF1; BID; CASP2; CASP6; CASP8; CASP10; CFLAR; CYCS; FAS; HSPB1; HTRA2; IKBKG; MAP4K4; MAPK8; RELA; TANK; TNFRSF21; TNFRSF10B; TNFRSF1A; TNFSF10; XIAP
ERK/MAPK Signaling	ARAF; ATF2; ATF4; BRAF; CREB3L4; DUSP1; EIF4EBP1; ELF2; ELF3; FOS; H3F3A/H3F3B; HRAS; HSPB1; ITGA2; ITGB1; KRAS; MKNK2; MRAS; MYC; NRAS; PAK2; PIK3C2A; PIK3CA; PIK3CD; PIK3R1; PIK3R2; PIK3R3; PLA2G12A; PLA2G12B; PLCG1; PPARG; PPP1CB; PPP1R7; PPP1R14B; PPP2R1B; PPP2R2A; PPP2R2C; PPP2R5A; PPP2R5C; PRKACB; PRKCA; PRKCI; PTK2; RPS6KA1; RPS6KA5; RRAS2; SOS1; SOS2; SRC; SRF; STAT1; STAT3; VRK2; YWHAB; YWHAQ
Ovarian Cancer Signaling	AKT1; AKT2; BRAF; CTNNB1; E2F1; FZD3; FZD4; FZD5; FZD6; FZD7; GSK3B; HNF1A; HRAS; KRAS; MRAS; MSH2; MSH6; NRAS; PA2G4; PGF; PIK3C2A; PIK3CA; PIK3CD; PIK3R1; PIK3R2; PIK3R3; PMS2; PRKACB; PTEN; RAD51; RB1; RRAS2; SIN3A; SRC; SUV39H1; TCF3; TCF7L2; TFDP1; TP53; VEGFA
FcγRIIβ Signaling in B Lymphocytes	AKT1; HRAS; KRAS; MAPK8; MRAS; NRAS; PDPK1; PIK3C2A; PIK3CA; PIK3CD; PIK3R1; PIK3R2; PIK3R3; RRAS2; SOS1
Estrogen Receptor Signaling	CCNH; CDK7; CTBP2; DDX5; GTF2H3; GTF2H4; GTF2H5; GTF2H2/LOC100510744; H3F3A/H3F3B; HNRNPD; HRAS; IGFBP1; KRAS; MED6; MED10; MED13; MED14; MED17; MED30; MED31; MED13L; MRAS; NCOA3; NR0B2; NR3C1; NRAS; PCK1; POLR2A; POLR2E; POLR2F; POLR2H; POLR2L; PPARGC1A; RRAS2; SOS1; SOS2; SRC; TAF3; TAF15; TAF4B; TAF9B
Endoplasmic Reticulum Stress Pathway	ATF4; ATF6; EIF2AK3; EIF2S1; ERN1; HSPA5; MAPK8; XBP1
Cleavage and Polyadenylation of Pre-mRNA	CPSF6; CSTF2; CSTF3; NUDT21; PABPN1; WDR33
IL-6 Signaling	CEBPB; CSNK2A1; CSNK2A2; FOS; HRAS; HSPB1; IKBKG; IL8; IL1R1; IL1RAP; IL6R; IL6ST; JUN; KRAS; MAP2K3; MAP2K6; MAP3K7; MAP4K4; MAPK8; MAPK13; MAPK14; MRAS; NRAS; RELA; RRAS2; SOS1; SOS2; SRF; STAT3; TNFRSF1A
IL-8 Signaling	AKT1; AKT2; ARAF; BCL2L1; BRAF; CCND3; CDH1; EIF4EBP1; FNBP1; GNA13; GNAS; GNB5; GNB2L1; GNG4; GPLD1; HBEGF; HRAS; ICAM1; IKBKG; IL8; IRAK2; KRAS; MAP4K4; MAPK8; MRAS; NAPEPLD; NRAS; PAK2; PGF; PIK3C2A; PIK3CA; PIK3CD; PIK3R1; PIK3R2; PIK3R3; PLD1; PRKCA; PRKCI; PRKD3; PTK2; RELA; RHOB; RHOQ; RHOT2; RHOU; ROCK1; ROCK2; RRAS2; SRC; VEGFA

Supporting Data S2 (Not shown). *Hierarchical clustering of significantly regulated genes.* The genes listed in Supporting Data S1 were clustered using Pearson correlation and average linkage in the MultiExperiment Viewer software. Expression values, here presented as fold change of control, from all time points, 8 and 14 hours +/- TNFα, and exposure conditions, diclofenac (DCF), carbamazepine (CBZ), ketoconazole (KTZ), nefazodone (NFZ) and methotrexate, (MTX) were used. The clusters identified as interesting (1-3) contained genes up-regulated after 8 hours DCF and CBZ exposure but down- or non-regulated after MTX treatment. The genes that could also be found to represent the interesting IPA®-defined canonical pathways presented in Figure 3 were labeled according to their respective pathways; yellow highlight = EIF2-signaling/Endoplasmic Reticulum Stress Pathway; green highlight = Nrf2-mediated Oxidative Stress Response; blue highlight = Apoptosis Signaling/Death receptor Signaling.

		HepG2, DCF 8h	Primary hepatocytes, mouse C57/BL6, DCF 24h	
Human symbol	Mouse symbol	FC	FDR	FC
SQSTM1	Sqstm1	4.14	0.043	1.27
SRXN1	Srxn1	2.08	0.014	2.27
DDIT3	Ddit3	8.14	0.001	2.54
TNFRSF10B	Tnfrsf10b	2.78	0.005	1.41
ATF4	Atf4	1.7	0.086	1.15
XBP1	Xbp1	1.33	0.007	-1.22
DNAJB6	Dnajb6	1.55	0.064	1.35
ABCC4	Abcc4	1.54	0.014	3.15
DNAJB1	Dnajb1	1.67	0.022	1.22
HSPA5	Hspa5	-1.6	0.001	1.44
ATF6	Atf6	1.42	0.043	1.20
SOD2	Sod2	3.16	0.054	-1.18
EIF4A1	Eif4a1	1.84	0.020	1.14
TRIB3	Trib3	5.6	0.002	2.02
PPP1R15A	Ppp1r15a	2.53	0.004	2.06

Supporting Data S3. *Genes downstream of oxidative and endoplasmic reticulum stress are significantly regulated in primary mouse hepatocytes.* Primary hepatocytes from C57BL/6 mice were treated with 300 M diclofenac for 24 h before mRNA collection and gene expression analysis. The expression of a selected number of genes, also regulated in HepG2 cells after 8 hours of DCF, downstream of Nrf2-dependent oxidative stress signaling and endoplasmic reticulum stress signaling, was determined. Only the genes that were significantly regulated, false discovery rate (FDR) < 0.1, are presented. Genes related to ER/translational stress are highlighted in orange and Nrf2-related genes in green.

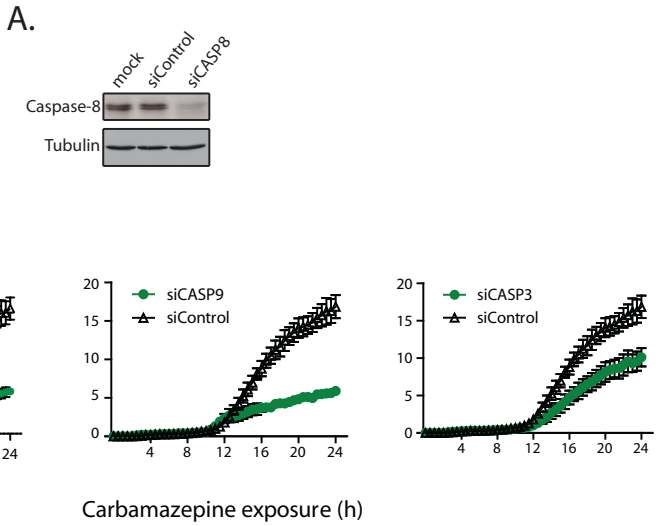

Supporting Data S4. *Knockdown of apoptosis related genes reduce CBZ/TNFα-induced apoptosis.* (A) Knockdown using SMART-pool siRNA targeting caspase-8 was confirmed using western blotting. Tubulin was used as loading control. (B) The apoptosis induced by CBZ/TNFα was followed in time using live cell imaging of apoptosis after SMARTpool siRNA mediated knockdown of Bcl2-family member BID, executioner caspase-3 and initiator caspase-9. TNFα (10 ng/mL) was added after 8 hours of drug exposure. Data presented are means of three independent experiments +/- S.E.M.

	siRNA	CBZ (p-value)	DCF (p-value)	Validation (CBZ)
Gene array	HERPUD1	> 0.05	n.a.	n.a.
	DNAJB1	< 0.001	> 0.05	2/4
	EIF4A2	> 0.05	n.a.	n.a.
	EIF4A1	< 0.001	< 0.001	4/4
	ATF4	> 0.05	n.a.	n.a.
	Bim/BCL2L11	< 0.001	Fredriksson *et al.*	2/4
	FOS	> 0.05	n.a.	n.a.
	JUN	> 0.05	n.a.	n.a.
	MCL1	> 0.05	n.a.	n.a.
	SQSTM1	> 0.05	n.a.	n.a.
	TNFRSF10B	> 0.05	n.a.	n.a.
	XIAP	> 0.05	n.a.	n.a.
	APAF1	< 0.001	Fredriksson *et al.*	3/4
	JUND	< 0.001	< 0.001	3/4
	BACH1	< 0.05	< 0.05	3/4
	KRAS	> 0.05	n.a.	n.a.
	SOD2	> 0.05	n.a.	n.a.
	SOS1	> 0.05	n.a.	n.a.
	CASP10	< 0.001	Fredriksson *et al.*	1/4
	DNAJB6	> 0.05	n.a.	n.a.
	EIF4G3	< 0.001	< 0.01	3/4
	PIK3C2A	> 0.05	n.a.	n.a.
	MRP4/ABCC4	< 0.001	< 0.001	3/4
	GSTO2	< 0.01	< 0.001	2/4
Apoptosis	CASP8	< 0.001	Fredriksson *et al.*	4/4
	CASP3	< 0.001	Fredriksson *et al.*	4/4
	CASP9	< 0.001	Fredriksson *et al.*	2/4
	BID	< 0.001	Fredriksson *et al.*	2/4
ER stress	CHOP/DDIT3	< 0.001	< 0.05	2/4
	PERK/EIF2AK3	< 0.01	< 0.05	4/4
	IRE1α/ERN1	< 0.001	< 0.001	2/4
	ATF6	< 0.001	< 0.001	2/4
Oxidative stress	SOD1	> 0.05	n.a.	n.a.
	GSR	< 0.001	< 0.001	2/4
	GPX4	< 0.001	< 0.001	3/4
	KEAP1	< 0.001	< 0.001	2/4
	NRF2	< 0.001	< 0.001	3/4

Supporting Data S5. *List of siRNAs and their effect on apoptosis following CBZ and DCF exposure.* HepG2 cells were transfected with siRNAs targeting genes up-regulated after 8 hours of CBZ and/or DCF exposure and involved in apoptosis/death receptor signalling (blue highlights), Nrf2-mediated oxidative stress response (green highlights) or ER stress/translation initiation (yellow highlights), and hand-picked from the three respective pathways. 72 hours after transfection the cells were exposed to CBZ (500 µM) with 10 ng/mL TNFα added after 8 hours of drug exposure and the apoptosis was assessed using AnxV-labelling and automated microscopy. The siRNAs that gave a significant difference in apoptosis compared to siControl (using 2-way ANOVA) were also assessed under DCF (500 µM)/TNFα-exposure conditions. The effect of the siRNAs found significant after CBZ exposure was also validated using the 4 single siRNA sequences that consisted the initial SMART-pool. A knockdown effect that could be confirmed with ≥ 2 of the single sequences (AUC = siControl ± 2-3 S.D.) was considered "on target".

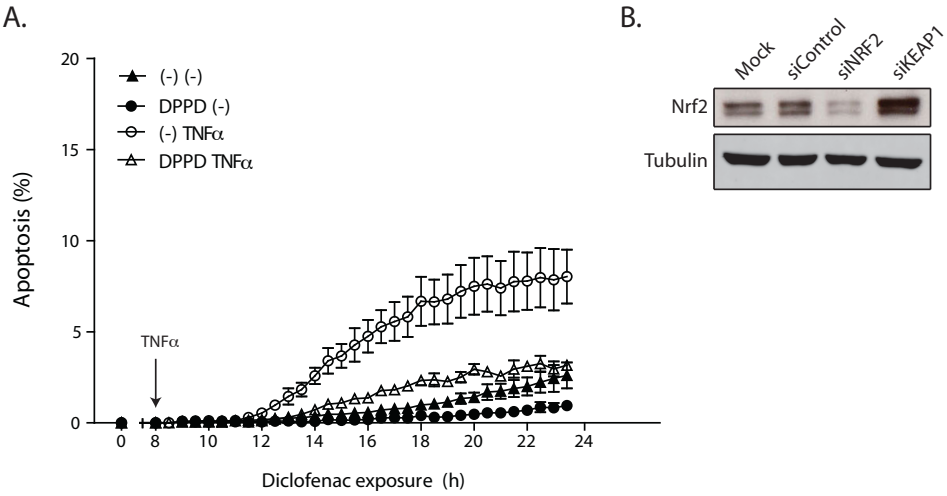

Supporting Data S6. *Modulation of the oxidative stress response.* (A) HepG2 cells were pre-treated with 10 µM N,N'-diphenylbenzene-1,4- diamine (DPPD) before adding 500 µM DCF or vehicle. TNFα (10 ng/mL) was added after 8 hours of drug exposure. The apoptosis induction was followed in time using AnnexinV (AnxV)-Alexa633 and automated microscopy. Data presented are means of three independent experiments +/- S.E.M. (B) Effect of NRF2 and KEAP1 siRNA-mediated knockdown on Nrf2 protein levels was assessed using westernblotting. Tubulin served as loading control.

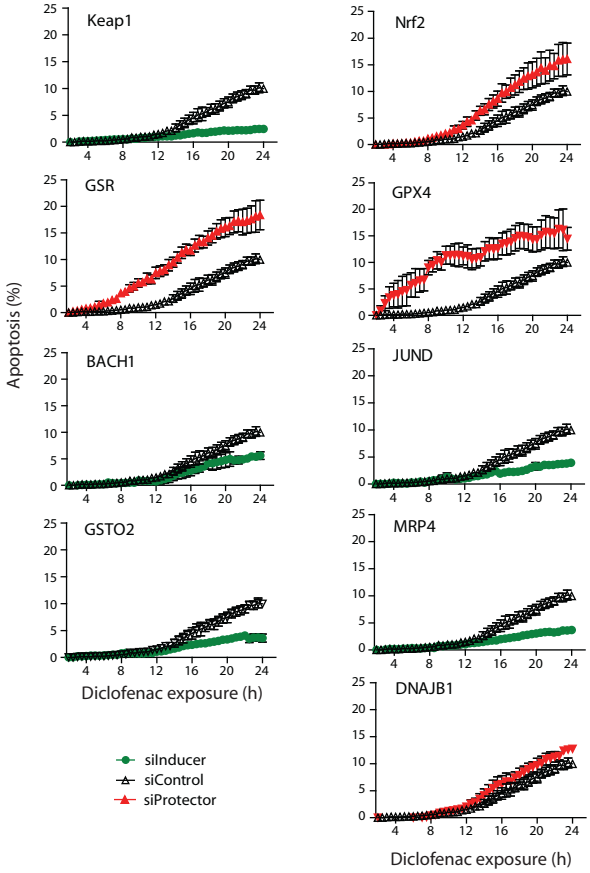

Supporting Data S7. *Knock-down of oxidative stress related genes affects apoptosis induced by DCF/TNFα.* The apoptosis induced by DCF/TNFα was followed in time using live cell imaging of apoptosis after SMARTpool siRNA mediated knockdown of genes involved in oxidative stress and found to give a significant effect on CBZ/TNFα-induced apoptosis. TNFα (10 ng/mL) was added after 8 hours of drug exposure.

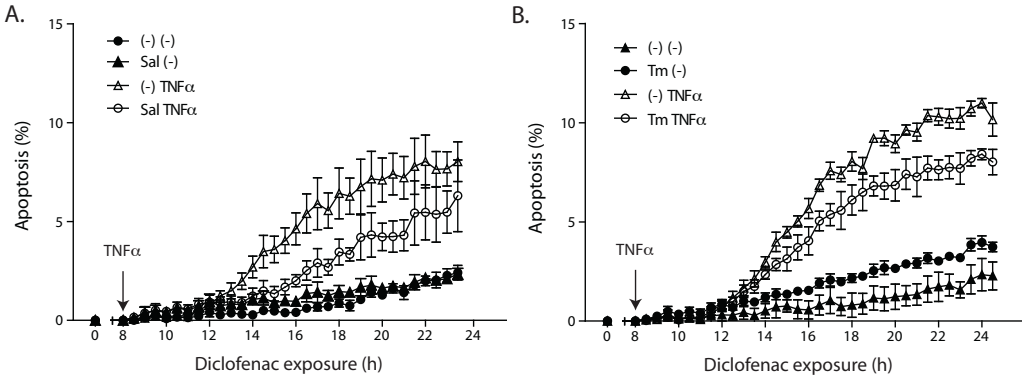

Supporting Data S8. *Inhibition of endoplasmic reticulum stress reduces DCF/TNFα-induced apoptosis.* HepG2 cells were pre-treated with 50 µM Salubrinal (Sal; A) or 5 µg/mL tunicamycin (Tm; B) before replacing the medium with 500 µM DCF. Salubrinal was kept in the medium where indicated. After 8 hours of DCF exposure, TNFα (10 ng/mL) was added. The apoptosis was determined in time using AnnexinV (AnxV)-Alexa633 staining and automated imaging. Data presented are means of three independent experiments +/- S.E.M.

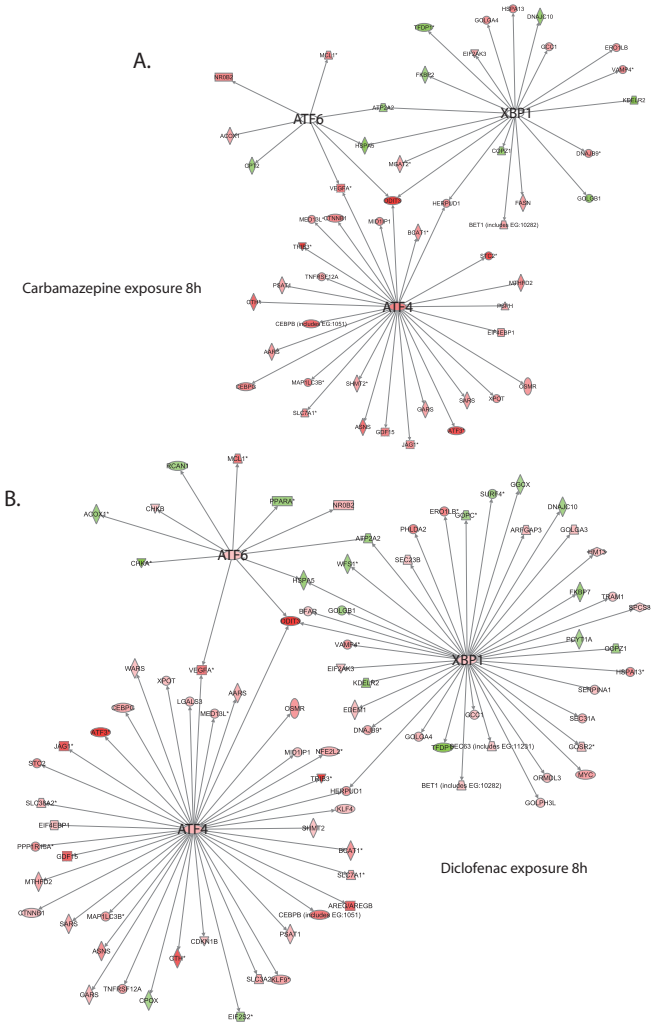

Supporting Data S9. *DCF and CBZ exposure induced mainly ATF4 mediated transcription.* Using the IPA® software the genes up- or down-regulated by the transcription factors downstream of the three distinct unfolded protein response pathways, PERK (ATF4), IRE-1α (XBP1) and ATF6 were determined after 8 hours DCF (A) or CBZ (B) exposure. Red colouring of the shapes indicate up-regulation of the target genes, while green indicated down-regulation. The intensity reflects the fold-change gene expression compared to vehicle-exposed cells.

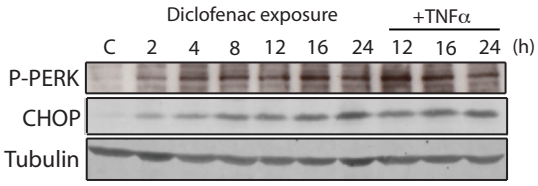

Supporting Data S10. *DCF induces PERK phosphorylation and CHOP expression.* The expression of phosphorylated PERK (P-PERK) and CHOP were followed in time by western blot after DCF+/- TNFα (500 µM/10 ng/mL) exposure.

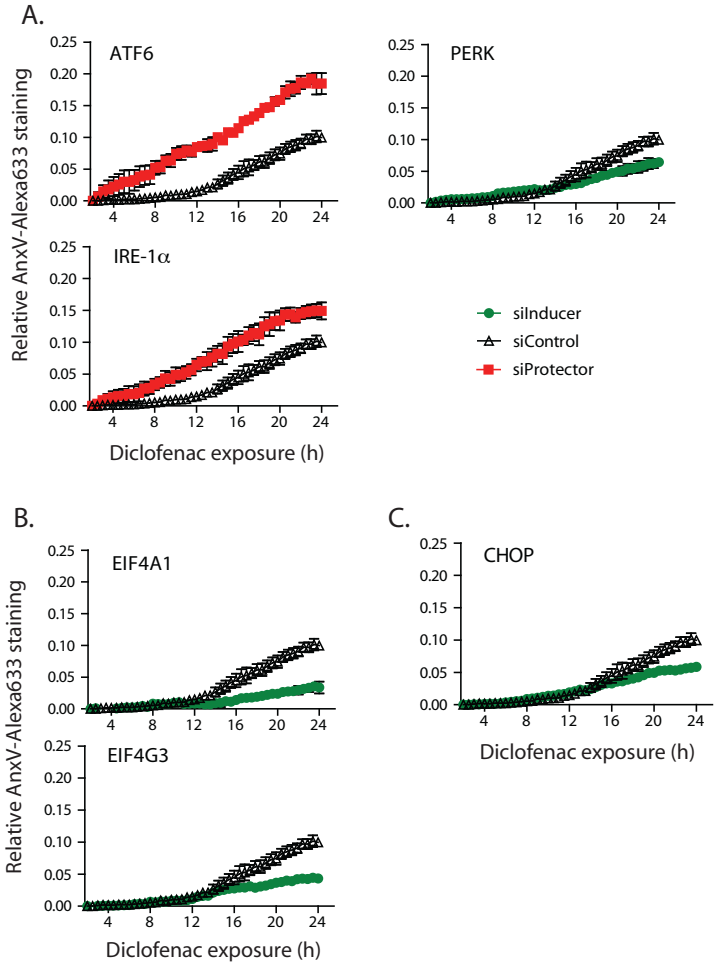

Supporting Data S11. *Knockdown of ER stress related genes affects apoptosis induced by DCF/TNFα.* (A-C) The apoptosis induced by DCF/TNFα was followed in time using live cell imaging of apoptosis after SMARTpool siRNA mediated knockdown of genes involved in ER stress and found to give a significant effect on CBZ/TNFα-induced apoptosis. TNFα (10 ng/mL) was added after 8 hours of drug exposure. Data presented are means of three independent experiments +/- S.E.M.